ELSEVIER

Journal of Structural Geology 27 (2005) 948–963

JOURNAL OF STRUCTURAL GEOLOGY

www.elsevier.com/locate/jsg

Rheological behaviour of synthetic rocksalt: the interplay between water, dynamic recrystallization and deformation mechanisms

J.H. Ter Heege*, J.H.P. De Bresser, C.J. Spiers

High Pressure and Temperature Laboratory, Faculty of Earth Sciences, Utrecht University, P.O. Box 80021, 3508 TA Utrecht, The Netherlands

Received 21 September 2004; accepted 4 April 2005
Available online 24 June 2005

Abstract

The ductile deformation of rocks in nature can be greatly enhanced by the presence of water. Part of the water-induced weakening of rocks at depth may come from fluid-assisted deformation or recrystallization mechanisms that are absent in dry rocks. In this study, we investigate the effect of water on the rheological behaviour of rocksalt. We focus on quantification of the contribution of individual deformation and recrystallization mechanisms to deformation. We also aim to calibrate a flow law that incorporates the effect of all the relevant microphysical processes and hence more accurately describes the flow of rocksalt in nature. For this purpose, the mechanical behaviour and microstructural evolution of synthetic rocksalt samples that are similar, except for differences in water content (determined using FTIR analysis), are investigated. The samples are deformed to natural strains of 0.07–0.46 at 50 MPa confining pressure, strain rates of 5×10^{-7}–1×10^{-4} s^{-1} and temperatures of 75–240 °C, resulting in flow stresses of 7–22 MPa. The flow stress of samples with a water content below ~5 ppm ('dry') is higher than that of samples with a water content of ~9–46 ppm ('wet') at all strains under the investigated conditions. The difference in flow stress can be explained as due to the operation of only work hardening dislocation creep without dynamic recrystallization in the dry material versus combined dislocation and solution-precipitation creep plus fluid-assisted grain boundary migration in the wet material. The results allow us to calibrate a flow law for wet rocksalt that incorporates the effects of solution-precipitation creep and fluid-assisted grain boundary migration. The results also suggest that strain localization in natural rocksalt is more likely to be localized due to fluid infiltration and associated rheological weakening, than due to progressive removal of strain hardening substructure by grain boundary migration.

Keywords: Rocksalt; Water; Dynamic recrystallization; Flow law

1. Introduction

Water plays a key role in controlling the ductile behaviour of rocks in the Earth's crust and mantle via a variety of weakening effects. Water weakening of ductile rock materials is usually related to (1) intracrystalline effects on dislocation mobility or lattice diffusion, or (2) intercrystalline effects such as enhanced grain boundary diffusion, enhanced grain boundary sliding, or solution-precipitation effects (e.g. Carter et al., 1990). Solution-precipitation effects, for example in solution-precipitation creep or grain boundary migration, are known to be particularly important in rocksalt and other salt minerals such as bischofite and carnallite (Urai, 1983, 1985; Urai et al., 1986).

Numerous studies have been performed to investigate the rheological behaviour of rocksalt at temperatures up to 250 °C (e.g. Heard, 1972; Wawersik and Zeuch, 1986; Carter et al., 1993; Franssen, 1994; Hunsche and Hampel, 1999). These studies generally indicate that deformation of rocksalt occurs by work hardening crystal plastic flow, at least at the faster strain rates and lower temperatures in the range of investigated conditions (e.g. above $\sim10^{-7}$ or 10^{-5} s^{-1} for 100 or 250 °C, respectively, Heard, 1972). There is some indication that mechanical steady state is achieved for slower strain rates and higher temperatures in such experiments, as the flow stress approaches a constant value at strains of 10–15%. However, few experiments have been performed beyond ~15% strain to investigate if

* Corresponding author. Present address: Institute for Geology, Mineralogy and Geophysics, Ruhr-University Bochum, D-44780 Bochum, Germany. Tel.: +49 234 322 5909; fax: +49 234 321 4181.
E-mail address: jan.terheege@ruhr-uni-bochum.de (J.H. Ter Heege).

0191-8141/$ - see front matter © 2005 Elsevier Ltd. All rights reserved.
doi:10.1016/j.jsg.2005.04.008

true mechanical and microstructural steady state is reached. Moreover, the effect of water was not systematically investigated in previous studies. It has been shown for wet rocksalt deforming at 125 °C and a strain rate of $\sim 5 \times 10^{-7}$ s^{-1} that strains of 5–10% are insufficient to initiate dynamic recrystallization and that much higher strains are required to achieve true mechanical and microstructural steady state (Watanabe and Peach, 2002). It has also been found that water (0.05 wt%) can create thin aqueous grain boundary films that facilitate solution, precipitation and diffusion processes, so that fine-grained rocksalt containing water deforms by solution-precipitation creep (Urai et al., 1986; Spiers et al., 1990). Furthermore, water can promote dynamic recrystallization by fluid-assisted grain boundary migration in rocksalt undergoing dislocation creep, provided that the mean stress is high enough to suppress grain boundary dilatation (Peach et al., 2001). Besides these processes related to water in grain boundaries, water might also be incorporated in grains, mainly in fluid inclusions that have been left behind during grain boundary migration and mark the original position of grain boundaries (Urai et al., 1986). Little water is incorporated in the crystal lattice of rocksalt (Carter et al., 1990). Microstructural observations during static recrystallization of synthetic rocksalt containing saturated brine reveal a direct relation between the mobility of grain boundaries and the presence of grain boundary fluid films (Schenk and Urai, 2004). In natural rocksalt, water is generally present (Roedder, 1984) and evidence for dynamic recrystallization by fluid-assisted grain boundary migration is widespread (Urai et al., 1986, 1987; Talbot and Jackson, 1987; Miralles et al., 2000). Therefore, a flow law for rocksalt that accounts for the effect of fluid-assisted grain boundary migration is crucial for developing a realistic rheological description of salt flow under natural conditions. However, no such flow law presently exists. Also it is not clear how important solution-precipitation creep may be relative to dislocation creep in determining the rheology of dynamically recrystallizing rocksalt in nature.

A realistic description of salt flow including the effect of fluid-assisted grain boundary processes is needed for accurate modelling of salt tectonic flow during basin evolution, and associated hydrocarbon generation, migration and trapping. It is also needed for modelling salt flow and resulting subsidence around deep solution-mining operations, for modelling borehole closure and for modelling the performance of storage and disposal facilities sited in rocksalt formations (e.g. Carter and Hansen, 1983; Peach, 1991; Aubertin and Hardy, 1998 and references therein).

In this study, we aim to obtain a mechanism-based description of the effects of water on deformation processes and rheology that can be extrapolated to model the flow of rocksalt under natural conditions. Therefore, we derived the first composite flow law for rocksalt under conditions where dislocation creep is influenced by dynamic recrystallization involving fluid-assisted grain boundary migration. We also determined the contribution of solution-precipitation creep to the overall creep rate to illustrate its importance during flow of rocksalt.

2. Experimental methods

Dense (>99.5% of theoretical density), translucent, cylindrical samples of polygonal-textured rocksalt were produced by cold-pressing analytical grade NaCl powder containing less than 0.1 wt% water and subsequent annealing for 1 week at 150 °C and 100 MPa confining pressure. This procedure yielded samples with initially 37–296 ppm water (Table 1) and an arithmetic mean grain size of 145 μm ('wet samples'). Selected samples were slowly heated ($\sim$0.1 °C/min) in flowing argon gas and held at 515 °C for $\sim$24 h, yielding samples with a water content of $\leq$5 ppm ('dry samples'). Dry and wet samples were deformed to natural strains of 0.3–0.7 at constant strain rates of 5.0×10^{-7}–1.3×10^{-4} s^{-1}, temperatures of 75–240 °C (0.33–0.50T/T_m) and a confining pressure of 50 MPa using two different silicone oil medium triaxial testing machines (Peach and Spiers, 1996; Watanabe and Peach, 2002; Ter Heege et al., 2005). Microstructures and grain size distributions of all samples were analysed using reflected light microscopy performed on polished and etched sections. Grain size was calculated in terms of equivalent circular diameters (ECD), without making any stereological correction for sectioning effects. For selection of samples, the ECD frequency distribution (referred to as the grain size distribution) and the distribution of area fraction occupied by a given ECD class (referred to as area distribution) are presented in a combined frequency histogram.

Water contents of the near-transparent samples were determined before and after the experiments using a Fourier transform infrared (FTIR) spectrometer (Magna 860, Nicolet). Infrared absorbance spectra were measured for wavenumbers of 1000–4000 cm^{-1}. The measurements were made on whole samples, in the axial or diametric directions, by directing the infrared beam through polished locations on the sample surface. Whole sample water contents were calculated from the peak area below the absorbance band at a wavenumber of 1650 cm^{-1}, which corresponds to the bending vibration of the water molecule in a saturated NaCl solution. The peak area was calibrated for water content using data obtained for a sample that was subsequently analysed using thermogravimetric analysis. Details on sample preparation, the deformation equipment and analysis methods can be found in previous papers (Peach and Spiers, 1996; Watanabe and Peach, 2002; Ter Heege et al., 2005). Water contents, measured after the experiments, are lower than the initial values measured soon after preparation (Table 1). It is unclear when and how the water loss occurred. It is unlikely that samples progressively dry out during the experiments by water loss from the

Table 1
Characteristics of the experiments and water contents of the rocksalt samples

Test[a]	First stress peak (MPa)	Strain at peak	First stress min. (MPa)	Strain at min.	Max. weak.[b] (MPa)	Flow stress[c] (MPa)	Strain rate[c] (s^{-1})	T^c (°C)	Nat. strain	Experimental duration (h)	H_2O cont. before (ppm)	H_2O cont. after (ppm)
Starting	–	–	–	–	–	–	–	–	–	–	–	–
p40t109dry[d]	–	–	–	–	–	19.7	5×10^{-7}	125	0.25	144.3	–	~5
15RS175dry	–	–	–	–	–	15.0	7.2×10^{-7}	167	0.51	329.8	–	~5
p40t115[d]	–	–	–	–	–	11.1	5×10^{-7}	125	0.07	43.8	196	32
p40t112[d]	12.5	0.10	–	–	–	12.4	5×10^{-7}	125	0.12	72.5	133	28
p40t114[d]	10.8	0.10	10.2	0.14	5.6	10.9	5×10^{-7}	125	0.25	144.0	257	36
p40t111[d]	11.8	0.09	11.3	0.13	4.2	11.8	5×10^{-7}	125	0.25	143.0	290	36
7RS150	4.8	0.07	–	–	–	7.2	5.3×10^{-7}	149	0.29	180.9	37	20
7RS200	6.7	0.10	–	–	–	7.5	2.4×10^{-6}	203	0.30	40.8	–	22
7RS240	7.1	0.10	6.8	0.12	4.2	7.3	1.6×10^{-5}	243	0.33	6.9	–	22
10RS240	9.9	0.14	9.0	0.20	9.0	9.5	1.3×10^{-4}	243	0.34	0.9	–	19
11RS125	9.9	0.07	9.6	0.10	3.0	10.8	5.4×10^{-7}	121	0.31	187.4	37	23
11RS150a	10.8	0.10	10.0	0.13	7.4	11.3	2.2×10^{-6}	150	0.31	45.1	–	30
11RS150b	10.7	0.10	10.4	0.13	2.8	11.3	1.4×10^{-6}	150	0.30	71.3	58	24
11RS175	11.6	0.11	10.3	0.18	11.2	10.9	6.6×10^{-6}	174	0.30	14.9	–	12
11RS200	12.0	0.20	11.1	0.36	7.5	11.1	2.4×10^{-5}	202	0.36	5.1	–	9
13RS125	13.1	0.11	12.3	0.14	6.1	13.3	1.3×10^{-6}	125	0.30	73.2	–	45
13RS150	13.6	0.16	12.7	0.23	6.6	13.3	4.5×10^{-6}	150	0.32	21.8	58	30
14RS100	14.3	0.13	13.0	0.17	9.1	13.6	5.3×10^{-7}	99	0.29	182.6	–	33
14RS150	14.4	0.14	13.3	0.20	7.6	14.4	6.6×10^{-6}	150	0.32	16.0	117	25
14RS175	15.3	0.26	13.9	0.44	9.2	13.9	5.0×10^{-5}	171	0.44	3.0	–	9
18RS100	20.4	0.18	17.8	0.27	12.7	17.9	2.8×10^{-6}	100	0.29	34.4	–	46
18RS125	20.3	0.20	17.6	0.31	13.3	17.7	7.4×10^{-6}	126	0.34	14.6	–	36
18RS150	18.8	0.19	17.0	0.31	9.6	17.6	3.6×10^{-5}	148	0.46	4.5	–	13
19RS150	19.3	0.23	18.8	0.31	2.6	19.1	4.5×10^{-5}	149	0.68	6.0	–	16
22RS75	24.0	0.23	21.6	0.32	10.0	21.7	5.4×10^{-7}	75	0.32	197.9	–	46
22RS100	26.0	0.25	22.1	0.37	15.0	22.1	7.5×10^{-6}	99	0.38	17.1	–	10
22RS150	22.4	0.32	–	–	–	22.4	3.2×10^{-5}	149	0.32	3.3	–	28

[a] Stress (first number) and temperature (second number) are quoted in most of the test numbers.
[b] Maximum weakening is calculated by $((\sigma_{peak}-\sigma_{min})/\sigma_{peak})\times100\%$ with σ_{peak} and σ_{min} the stress peak and subsequent minimum.
[c] Flow stress, strain rate and temperature (T) averaged over a strain of 0.01 at the end of the test.
[d] Experiments from Watanabe and Peach (2002).

jackets, as the lowest water contents do not correlate with test duration or temperature (i.e. samples deformed in the longest experiments or experiments at highest temperature do not necessarily show the lowest water contents). Moreover, a change from 'wet behaviour' to much stronger 'dry behaviour' has not been observed as would be expected if samples progressively dried out during the experiments. Instead, we believe that the sample water content evolved to a background level of 10–40 ppm during storage prior to testing (or prior to drying in the case of the dry samples). We accordingly take the final water content as indicative of the water present in the samples (at grain boundaries or inside grains) during the experiments.

3. Results

3.1. Mechanical behaviour

The details of all experiments performed are listed in Table 1. Typical stress–strain data at constant strain rate (~5–$7\times10^{-7}\,s^{-1}$) or at roughly constant stress (~11 MPa) and temperature (150 °C) are depicted in Fig. 1a and b, respectively.

The dry aggregates show continuous work hardening up to a strain of 0.25–0.51 at a strain rate of 5–$7\times10^{-7}\,s^{-1}$ and temperatures of 125 and 175 °C without reaching a steady-state flow stress. The wet aggregates show work hardening as well, but only to natural strains of 0.07–0.32 and at a lower rate than the dry samples. A general feature of the experiments on the wet samples is the oscillating stress–strain behaviour with local (broad) stress peaks followed by stress minima (Fig. 1a and b). Two types of stress–strain curves can be identified for the wet samples deformed to natural strains of 0.3–0.4:

(1) Curves with a peak or plateau in flow stress, followed by a stress minimum and subsequent strain hardening to a second peak at a higher stress (e.g. 7RS150, 7RS240 and 11RS125). This type of mechanical behaviour occurs at low strain rates and relatively high temperatures.

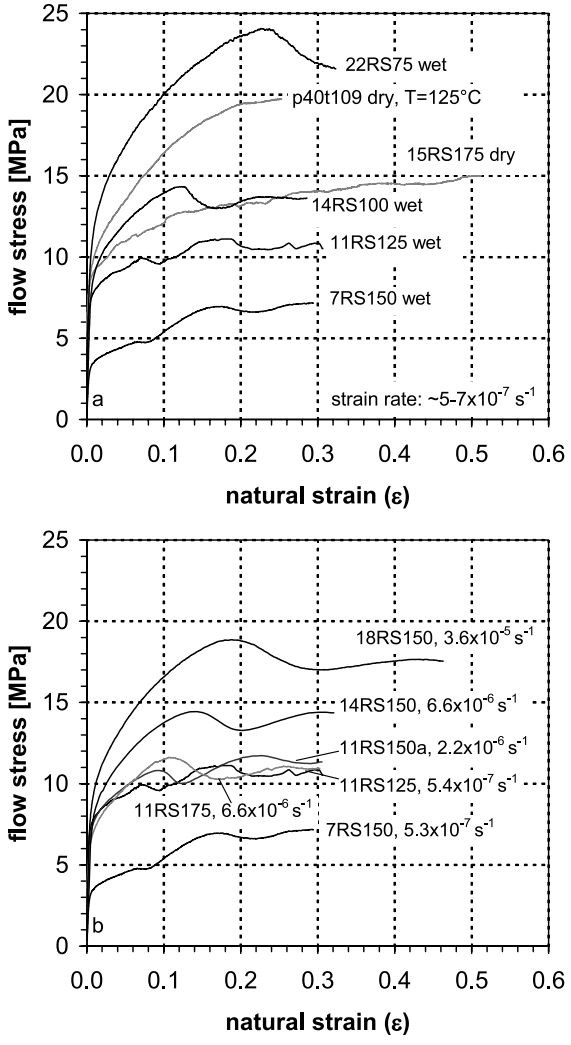

Fig. 1. Typical stress–strain curves showing the effect of temperature (75–175 °C, indicated in sample number) at $\dot{\varepsilon} \approx 5\text{–}7 \times 10^{-7}$ s^{-1} (a) and strain rate (5.3×10^{-7}–3.6×10^{-5} s^{-1}) and stress at $T = 125$–175 °C (b) on the mechanical behaviour of wet rocksalt. For comparison, the two stress–strain curves for dry rocksalt ($T = 125$ and 175 °C) are included in (a).

(2) Curves with a peak in flow stress, followed by strain softening to a stress minimum and limited hardening to a second peak at a lower stress (e.g. 14RS100, 18RS150). This type of behaviour occurs at strain rates that are higher and temperatures that are lower than for type (1).

Note that at the highest stress investigated ($\sigma > 20$ MPa), the maximum strain achieved in the experiments is insufficient to reach a second stress peak (i.e. the oscillation pattern is incomplete). At the lower strain rates and relatively high temperatures, the stress–strain curves show at least two complete cycles of a peak stress followed by a stress minimum. The difference between stress peaks and subsequent minima decreases with increasing strain, yielding a near steady-state flow stress at high strains (e.g.

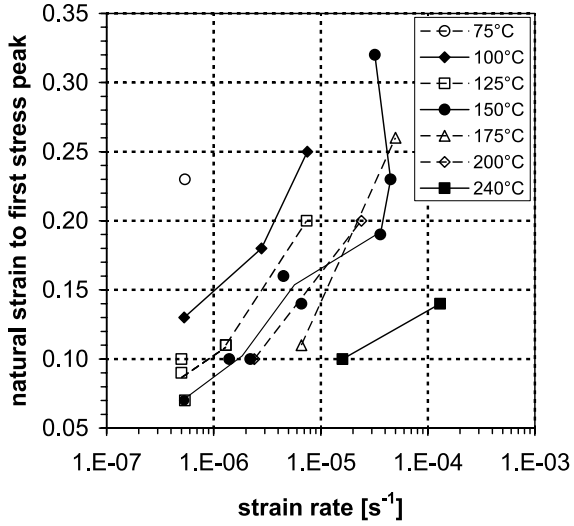

Fig. 2. Natural strain required to reach the first stress peak versus strain rate for wet rocksalt deformed at different temperatures.

11RS175, 14RS100 and 18RS150). The strain required to reach the first stress peak increases with decreasing temperature and increasing strain rate (Fig. 2, Table 1). The rheological weakening associated with the oscillations, calculated as the relative difference in stress between the stress peak and subsequent stress minimum (yielding the maximum weakening), also tends to increase with decreasing temperature and increasing strain rate (Fig. 3, Table 1). The weakening is below 15% in all experiments.

The stress versus strain rate data obtained for all experiments on wet and dry rocksalt are depicted in Fig. 4. The figure includes flow stresses averaged over the last 0.01 strain in the experiments as well as the stress

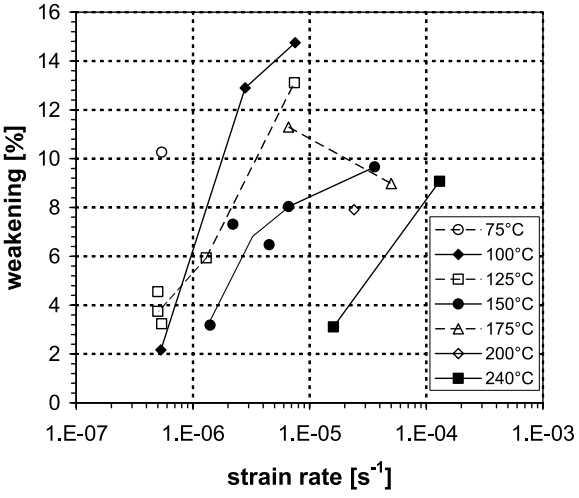

Fig. 3. Weakening due to the onset of fluid-assisted grain boundary migration recrystallization, calculated using $((\sigma_{peak} - \sigma_{min})/\sigma_{peak}) \times 100\%$ with σ_{peak} and σ_{min} being the stress peak and subsequent minimum (see Table 1) versus strain rate for wet rocksalt deformed at different temperatures.

maxima and subsequent minima in the experiments, which are added for comparison. Flow stresses increase with increasing strain rate and decreasing temperature at all conditions. Flow stresses exhibited by wet rocksalt are lower than flow stresses shown by dry rocksalt at all strains. The flow stresses for dry rocksalt at the end of the experiment are up to a factor ~2 higher than the flow stresses for wet rocksalt at the same conditions. For wet rocksalt, the strain rate ($\dot{\varepsilon}$) can be related to the flow stress (σ) using a Dorn-type power law equation

$$\dot{\varepsilon} = A\sigma^n \exp\left(\frac{-Q}{RT}\right) \quad (1)$$

Table 2 shows values for the rate constant A (in $MPa^{-n}\,s^{-1}$), stress exponent (n) and apparent activation energy (Q) obtained from a non-linear best fit of the data to Eq. (1). Only data of the last 0.01 strain in the experiments on wet rocksalt are used for the fit. In other words, the stress maxima and minima, indicated in Fig. 4, were not included in the analysis, so that the best fit represents a quasi steady-state description. Isotherms of Eq. (1) with the best fit values of $\log A = -1.56 \pm 0.54$, $n = 5.6 \pm 0.5$ and $Q = 80 \pm 6$ kJ/mol for the data on wet rocksalt are indicated in Fig. 4.

3.2. Microstructures and grain size distributions

The dry and wet rocksalt starting materials consist of equidimensional polygonal grains with no internal structure and straight or gently curved grain boundaries that often intersect at ~120° triple junctions (Fig. 5a). The grain size distribution is close to lognormal with a median and an arithmetic mean of 123 and 145 μm, respectively (Fig. 5b).

The microstructures of the wet deformed rocksalt show that just before the first stress peak (at a natural strain of ~0.07 at 125 °C, Fig. 5c), grains have flattened (average aspect ratio 1.31) and occasionally developed internal structure with linear and wavy etch features. Minor dynamic recrystallization has occurred, mainly by grain boundary migration, as evidenced by occasional grain boundary bulges (Fig. 5c). Grain boundaries preferentially align at 45° to the compression direction. Grain size has increased with respect to the starting material to 185 or 217 μm, for the median and arithmetic mean, respectively (Fig. 5d). Subgrains have developed, generally at grain boundaries or triple junctions. The subgrains are usually smaller than the grain boundary bulges (Fig. 5c). After the first stress peak, grains showing deformation substructures, such as subgrains or linear/wavy etch features (Fig. 5e), are partly replaced by dynamically recrystallized grains with little internal structure and idiomorphic grain boundaries. Dynamic recrystallization is dominated by grain-scale grain boundary migration, involving removal of grains with well-developed substructure as well as grain dissection. The grain size distributions show that grain boundary migration after the first stress peak results in a dramatic increase in median and arithmetic mean grain size (from 185 and 217 μm to 288 and 774 μm, respectively, at 125 °C). The microstructures and grain size distributions of the wet samples are described in more detail in a separate study (Ter Heege et al., 2005).

The dry deformed rocksalt sample studied shows a polygonal grain structure in which the grains have flattened considerably with respect to the starting material. This is indicated by a change in aspect ratio from 1.0 for the starting material to 1.5 for the dry deformed material at the investigated strain. Grain

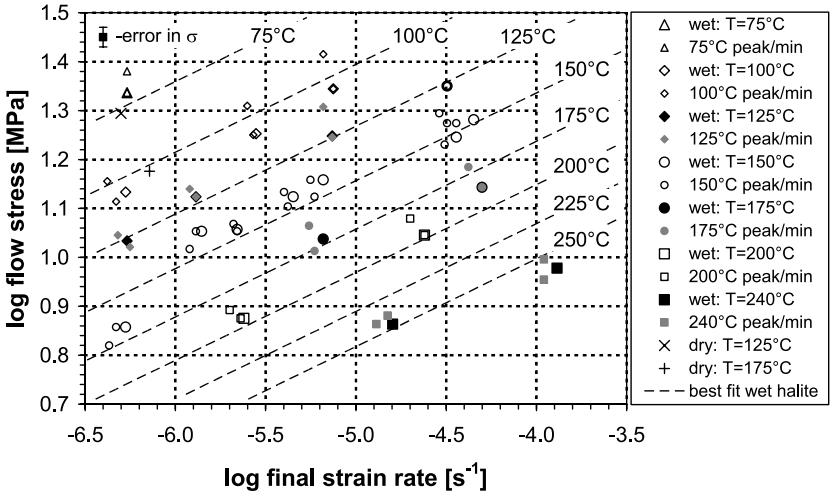

Fig. 4. Flow stresses for dry and wet samples of rocksalt at the end of the experiments (large symbols) and at stress maxima and subsequent minima (small symbols) for different strain rates and temperatures. Isotherms for a non-linear best fit of the flow stress at the end of the experiments on wet rocksalt to a power law creep equation (cf. Eq. (1)) are also indicated (dashed lines). In some cases, stresses at the end of the experiments are similar to stress maxima/minima and the symbols plot on top of each other (e.g. 13RS125).

Table 2
Power law creep parameters for rocksalt from this study and several other studies with deformation conditions, material source and water content of the samples

Material/ composition	H_2O (ppm)	P (MPa)	Strain rate (s^{-1})	Temperature (°C)	Stress (MPa)	$-\log(A)$ ($MPa^{-n}\,s^{-1}$)	Stress exponent	Q (kJ/mol)	Source/ comments
Synthetic pure rocksalt	9–46	50	10^{-4}–10^{-7}	75–250	7.2–22.4	1.56±0.54	5.6±0.5	80±6	This study
Synthetic pure rocksalt	20–45	200	10^{-1}–10^{-8}	23–400	1.6–47	0.11±0.82	5.5±0.4	98±8	Heard (1972)
Synthetic pure rocksalt	20–45	200	10^{-1}–10^{-8}	23–400	1.6–47	0.7±0.4	5.8±0.2	96±3	Heard and Ryerson (1986)
Natural (>95% rocksalt)[a]	?	14, 21	10^{-6}–10^{-11}	23–160	8.3–24	3.36–6.03	4.1–6.3	50–83	Wawersik and Zeuch (1986)
Natural (>99% rocksalt)[b]	<100	2.5–20.7	10^{-6}–10^{-9}	50–200	6.9–20.7	3.80	5.3±0.4	68±4	Carter et al. (1993)—high $\dot{\varepsilon}$, σ
Natural (>99% rocksalt)[b]	<100	2.5–20.7	10^{-7}–10^{-9}	100–200	2.5–10.3	4.09	3.4±0.1	52±1	Carter et al. (1993)—low $\dot{\varepsilon}$, σ
Synthetic pure rocksalt	Dry	Unconf.	10^{-3}–10^{-7}	250–780	0.4–14.8	0.76±0.02	5.7±0.3	129±8	Franssen (1994)—low T regime
Natural rocksalt[c]	?	Unconf.+ 15–20	10^{-3}–10^{-11}	30–250	1.7–40	–	7	110	Hunsche and Hampel (1999)[d]
Natural (>98% rocksalt)[c]	500	3–30	3.5×10^{-7}	150	11–13	–	–	–	Peach et al. (2001)

[a] Range of parameters for natural rocksalt from five different locations: Salado (New Mexico), West Hackberry and Bayou Choctaw (Louisiana), Bryan Mound (Texas) and Asse (Germany).
[b] Avery Island (Louisiana).
[c] Asse Speisesalz (Germany).
[d] In this study, mechanical data were fitted to a composite law. Stress exponent and activation energy quoted here are from their best fit to a power law equation (cf. Eq. (1)). Strain rates are compared (Fig. 7) using their composite law.

boundaries are generally straight or gently curved and often intersect at ~120° triple junctions (cf. starting material). There is no evidence for grain boundary migration in the dry samples. A substructure with linear etch features has developed in many grains (Fig. 5g). Parallel linear etch features are frequently bridged by features oblique to the main orientation, resulting in a wavy appearance of the etch features. In addition, subgrains are widespread within grain cores and at grain boundaries. In areas where the subgrain structure is well developed, the linear (wavy) etch features are usually absent. The grain size has increased slightly with respect to the starting material (median and arithmetic mean increase to 188 and 218 μm, respectively, at 125 °C, Fig. 5h).

4. Discussion

4.1. Flow behaviour in relation to microstructural evolution

The results show that dry samples of rocksalt exhibit continuous work hardening at the conditions investigated. Work hardening is accompanied by the development of a dislocation substructure revealed by etching in almost all grains. Beyond a strain of ~0.1, the work hardening rate decreases with increasing strain. This type of flow behaviour and microstructural evolution indicates that the dry samples are deformed by dislocation plastic mechanisms with increasing recovery towards high strain. We refer to this type of flow as work hardening dislocation creep, as steady state is not achieved under the investigated conditions and the dislocation substructure presumably continues to evolve in the approach to steady state. Accordingly, a (steady state) flow law cannot be calibrated for our dry samples. Previous studies on rocksalt reveal that the linear (wavy) substructure observed in the dry samples is caused by the cross slip of screw dislocations on {100} and {111} planes, bridging parallel {110} slip planes (Skrotzki and Liu, 1982; Senseny et al., 1992; Carter et al., 1993). Therefore, we conclude that at the investigated conditions, dislocation creep in dry rocksalt is probably controlled by the cross slip of screw dislocations, though this needs confirmation by electron microscopy studies. As no evidence for grain boundary migration was found, it is unclear what caused the apparent increase in grain size of the dry sample deformed to a strain of 0.25 with respect to the starting material. It most likely reflects variation in the starting material.

The results for the wet samples show that up to the first stress peak they behave similarly to the dry samples,

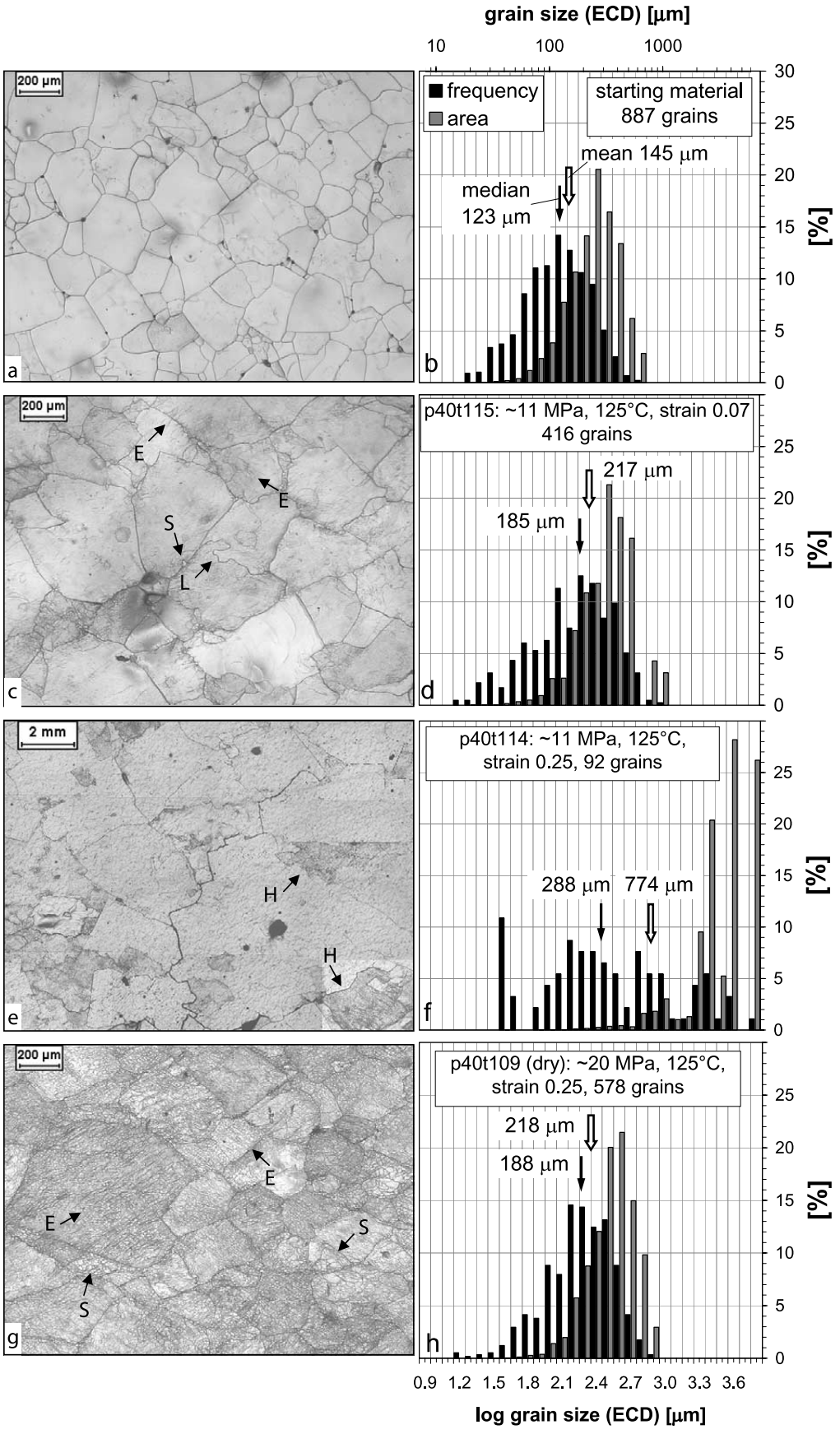
grain size (ECD) [μm]
10
100
1000
200 μm
frequency
area
starting material
887 grains
mean 145 μm
median
123 μm
[%]
a
b
200 μm
E
E
S
L
p40t115: ~11 MPa, 125°C, strain 0.07
416 grains
217 μm
185 μm
c
d
2 mm
H
H
p40t114: ~11 MPa, 125°C,
strain 0.25, 92 grains
288 μm
774 μm
e
f
200 μm
E
E
S
S
p40t109 (dry): ~20 MPa, 125°C,
strain 0.25, 578 grains
218 μm
188 μm
g
h
0.9 1.2 1.5 1.8 2.1 2.4 2.7 3.0 3.3 3.6
log grain size (ECD) [μm]

exhibiting work hardening flow and development of subgrain structure. However, the flow stress is lower than in the dry samples at all strains up to the first stress peak (cf. Fig. 1). The alignment of grain boundaries at ~45° to the compression direction probably results from a combination of grain boundary sliding and dislocation creep accompanied by minor grain boundary migration at triple junctions (Drury and Humphreys, 1988). Grain boundary migration initiates just before the first stress peak (Fig. 5c). Beyond this point, the wet samples show considerable weakening, followed by oscillations in flow stress. The grain boundary migration must be fluid-assisted, as evidenced by its absence in the dry samples. High grain boundary mobility is interpreted to be achieved by solution-precipitation transfer across thin fluid films at grain boundaries (Urai et al., 1986; Spiers and Carter, 1998; Peach et al., 2001; Schenk and Urai, 2004). The oscillations in flow stress can be explained by the interaction of recovery, work hardening and fluid-assisted grain boundary migration, leading to softening as relatively strain-free grains (low internal energy) replace highly substructured grains (high internal energy). Softening is then followed by hardening if most grains full of substructure have been replaced and the driving force for migration diminishes. This type of cyclic mechanical behaviour with oscillating flow stress is analogous to the mechanical behaviour of many metals (e.g. Sellars, 1978). It requires fast grain boundary migration as strain hardened grains need to be completely replaced by strain-free grains before ongoing deformation has again resulted in the development of strain hardening substructure. After several oscillations, the recrystallization process becomes out of phase throughout the material, leading to a dynamically stable balance between hardening and softening processes and a (near) steady-state flow stress (Sellars, 1978; Watanabe and Peach, 2002). At relatively low temperatures and high strain rates, the work hardening rate is high with respect to the grain boundary migration rate. In this situation, more strain is required to achieve a balance between hardening and softening and to reach the peak stress (Fig. 2, Table 1). Also, the amount of weakening due to grain boundary migration is higher than at relatively high temperature and low strain rate (Fig. 3, Table 1).

4.2. Effect of water on flow stress

Water contents analysed at the end of the experiments show that a critical amount of 9–46 ppm water is required for rocksalt to behave in a 'wet' manner and to undergo dynamic recrystallization by grain boundary migration. At water contents below ~5 ppm, rocksalt behaves in a 'dry' manner and grain boundary migration is inhibited. The widespread occurrence of fluid-assisted grain boundary migration in wet rocksalt indicates that a water content of 9–46 ppm is sufficient to wet virtually all grain boundaries and to facilitate solution-precipitation transfer across grain boundaries. We believe that the water content of 9–46 ppm can be viewed as an equilibrium amount left in our samples prior to testing and that it is enough to wet the grain boundaries. The fluid pressure during experiments is probably similar to the confining pressure in our experiments. We did not investigate the behaviour of rocksalt with water content between 5 and 9 ppm, but the change from 'dry' to 'wet' behaviour seems to occur abruptly within this interval, suggesting that amounts less than 9 ppm do not allow continuous wetting of grain boundaries.

In accordance with the above, the distinct difference in rheology and microstructural evolution between wet and dry rocksalt beyond the first stress peak can be attributed to the operation of fluid-assisted grain boundary migration. Before the first stress peak, samples show only minor grain boundary migration resulting in occasional grain boundary bulges and no evidence for widespread replacement of strain hardened grains by softer grains that are free of substructure (Fig. 5c). However, before the first stress peak the flow stress of the wet samples is also much lower than that for the dry samples, despite the absence of significant dynamic recrystallization. This difference indicates the operation of a process leading to water weakening independently of dynamic recrystallization. Potential candidates are enhancement of dislocation mobility (hydrolytic weakening) or solution-precipitation creep (Carter et al., 1990). We are aware of no evidence for an intracrystalline effect of water on dislocation mobility in rocksalt, so this option seems unlikely. However, solution-precipitation creep has been recorded previously in wet fine-grained halite (Urai et al., 1986; Spiers et al., 1990).

We will now investigate if the observed difference in flow stress between wet and dry rocksalt before the first stress peak can be quantitatively explained by the contribution of solution-precipitation creep to the overall creep rate of wet rocksalt. We use the following procedure:

(1) Stress–strain curves of two representative experiments on dry and wet rocksalt (p40t109 and p40t115, respectively),

Fig. 5. Microstructures of rocksalt starting material and wet and dry samples deformed by Watanabe and Peach (2002) to different strains at $T = 125$ °C and $\dot{\varepsilon} \approx 5 \times 10^{-7}$ s^{-1} with logarithmic grain size distributions (ECD, equivalent circular diameter). Median and arithmetic mean of ECD are indicated by arrows and/or numbers. (a) and (b) Undeformed starting material (wet and dry) showing equidimensional polygonal grains with no internal structure and straight or gently curved grain boundaries that often intersect at ~120° triple junctions. (c) and (d) Sample p40t115 (wet), just before the first stress peak, showing a lobate grain boundary (L), occasional linear etch features (E) and some subgrains at grain boundaries (S). (e) and (f) Sample p40t114 (wet) at the end of the experiment, showing a fully recrystallized microstructure with some grains exhibiting little internal structure and some grains with well developed internal structure (H). Many grain boundaries are straight (idiomorphic). (g) and (h) Sample p40t109 (dry) at the end of the experiment, showing grains with a well-developed subgrain structure (S), some wavy slip lines (E) and straight or gently curved grain boundaries that often intersect at ~120° triple junctions. Compression direction vertical in (e) and (g). Note that (e) and (g) were deformed to similar strain, but show a distinct difference in grain size (note different scale bars).

both deformed at $T = 125$ °C and $\dot{\varepsilon} = \sim 5 \times 10^{-7}$ s^{-1}, are taken for comparison between dry and wet behaviour (Fig. 6). After the experiment, sample p40t109 does not show evidence for significant dynamic recrystallization and associated change in grain size or for deformation mechanisms other than dislocation creep (Fig. 5g and h). Therefore, it is justified to assume that deformation is due to dislocation creep alone. Sample p40t115 was ended just before the first stress peak and microstructural observations indicated that at this point dynamic recrystallization has not significantly altered the microstructure (Fig. 5c). Without significant dynamic recrystallization in both samples, differences in mechanical behaviour between the two samples can be considered to result from differences in deformation mechanisms and not due to dynamic recrystallization. The stress–strain curve of p40t109 is taken as representative of dislocation creep in dry *and* wet rocksalt at the investigated conditions, i.e. it is assumed that water has no influence on the dislocation creep rate.

(2) The contribution of solution-precipitation creep in p40t115 is calculated using the well constrained flow law for solution-precipitation creep in dense rocksalt and the grain size distribution of p40t115. The solution-precipitation creep rate can be related to the flow stress by (Spiers and Carter, 1998)

$$\dot{\varepsilon}_{sp} = (4.7 \pm 2.3) 10^5 \frac{\sigma}{T d^3} \exp\left(\frac{-24.5 \pm 1.0}{RT}\right) \quad (2)$$

with the flow rate ($\dot{\varepsilon}_{sp}$) in s^{-1}, temperature (T) in K, stress (σ) in MPa, mean grain size (d) in μm and the gas constant (R) in kJ/mol. This flow law has been calibrated on the basis of experiments on porous and dense polycrystalline aggregates of synthetic rocksalt by Spiers et al. (1990).

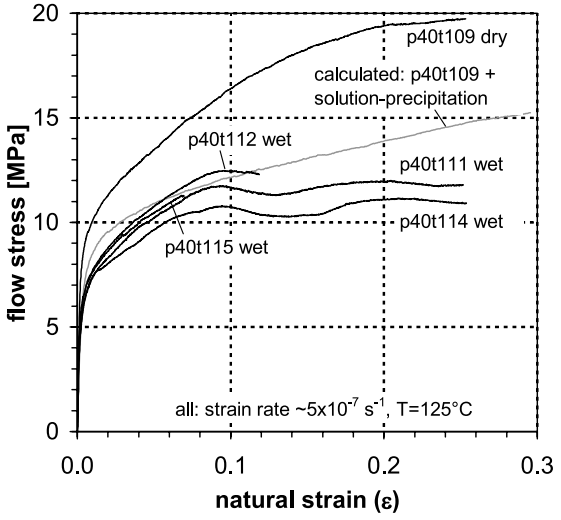

Fig. 6. Stress–strain curves for dry and wet rocksalt (p40t09–p40t115) deformed by Watanabe and Peach (2002) to different strains at $T = 125°$ and $\dot{\varepsilon} \approx 5 \times 10^{-7}$ s^{-1}. Also indicated is the stress–strain curve calculated by adding the (calculated) contribution of solution-precipitation creep to p40t109 (light grey).

Eq. (2) describes steady-state deformation by solution-precipitation creep. In fully dense aggregates deforming by solution-precipitation creep, steady-state deformation occurs once a stable structure has developed within grain contacts so that the average diffusive properties of the grain boundary fluid are constant. Electrical impedance measurements performed during experiment p40t115 show that resistivity does not change significantly for natural strains of 0.02–0.07, indicating that the average diffusive properties of the grain boundary fluid are indeed constant for these strains (Watanabe and Peach, 2002). Therefore, application of the steady-state flow law to calculate the contribution of solution-precipitation creep in p40t115 seems reasonable in any case beyond the first ~2% strain. In order to determine the strain due to solution-precipitation, we follow an approach comparable with the one used to determine the contribution of grain size sensitive mechanisms in deformation of Carrara marble with a distributed grain size (Ter Heege, 2002; Ter Heege et al., 2002). First, the number densities of each grain size class (i) in the grain size distribution (consisting of j classes) of p40t115 (Fig. 5d) are converted to volume fractions (v_i) using the Stripstar computer program (Heilbronner and Bruhn, 1998). Then, the solution-precipitation creep rate ($\dot{\varepsilon}_{sp}$) at a given stress is determined by volume averaging the strain rate in individual grain size classes ($\dot{\varepsilon}_i$), given by Eq. (2), assuming that stress is uniform in the aggregate ($\dot{\varepsilon}_{sp} = \dot{\varepsilon}_1 v_1 + \dot{\varepsilon}_2 v_2 + \cdots + \dot{\varepsilon}_j v_j$). The uniform stress assumption gives an upper bound for the rate of deformation in the aggregate (Raj and Ghosh, 1981; Freeman and Ferguson, 1986; Tullis et al., 1991; Ter Heege et al., 2004). A lower bound would be provided by assuming that strain rate is uniform in the aggregate. Volume averaging of the local stress in individual grain size classes due to combined dislocation and solution-precipitation creep mechanisms would then give the bulk flow stress. However, local stresses cannot be determined on the basis of the stress–strain curve of p40t109 and Eq. (2) and we are limited to the uniform stress approach. Within a time interval $\Delta t = t_{x+1} - t_x$, work hardening dislocation flow results in an increment of strain $\Delta\varepsilon = \varepsilon_{x+1} - \varepsilon_x$ and a stress increment $\Delta\sigma = \sigma_{x+1} - \sigma_x$, given by the stress–strain curve of p40t109 (Fig. 6). Using volume averaging of strain rate, the pressure solution creep rate in the same interval Δt can be approximated by calculating $\dot{\varepsilon}_{sp}$ at the average stress $\sigma_x^{av} = (\sigma_{x+1} - \sigma_x)/2$ in interval Δt (written as $\dot{\varepsilon}_{sp}(\sigma_x^{av})$ in the following). The strain increment due to solution-precipitation creep ($\Delta\varepsilon_{sp}$) over interval Δt is given by $\dot{\varepsilon}_{sp}(\sigma_x^{av})\Delta t$. The total amount of strain due to solution-precipitation creep (ε_{sp}) at a given stress (σ_x) can now be calculated by summing the strain increments calculated for each stress point on the stress–strain curve of p40t109 up to σ_x

$$\varepsilon_{sp} = \sum_1^x \Delta\varepsilon_{sp} = \sum_1^x \dot{\varepsilon}_{sp}(\sigma_x^{av})\Delta t \quad (3)$$

(3) A stress–strain curve for a combination of dislocation

creep and solution-precipitation creep is constructed by adding the calculated contribution of solution-precipitation creep, given by Eq. (3), and the stress–strain curve of p40t109 (Fig. 6). The stress–strain curve of the dry material shifts by ε_{sp} along the strain axis at a given stress σ_x^{av} as a result of the contribution of solution-precipitation creep to the overall deformation. It has to be noted that we use the flow law given by Eq. (2) to calculate the solution-precipitation strain rate in individual grain size classes ($\dot{\varepsilon}_i$), while the flow law is calibrated for bulk materials exhibiting a grain size distribution. The error introduced by applying Eq. (2) to individual grain size classes (i.e. terms describing grain size distribution characteristics incorporated in the pre-exponential terms in Eq. (2) are not accounted for) may be expected to be small compared to other uncertainties in the analysis (e.g. uniform stress assumption).

(4) The constructed stress–strain curve is compared with the actual stress–strain curve for wet rocksalt (p40t115) to evaluate if the stress difference between wet and dry rocksalt can be attributed to the effect of solution-precipitation creep. It can be seen that the constructed curve for combined dislocation and solution-precipitation creep is very close to the stress–strain curve of the wet sample p40t115, especially at the end of experiment p40t115. Differences between the calculated stress–strain curve and the curve for p40t115 might be caused by the fact that the final grain size distribution of p40t115 is used in the calculations, and not the evolution towards it. Note in this respect that the correspondence is indeed best at the end of p40t115. Under the assumptions adopted, the water weakening effect in rocksalt prior to the onset of dynamic recrystallization can thus be largely explained by the contribution of solution-precipitation creep to the overall strain rate. Other weakening mechanisms (e.g. intracrystalline) are not necessary to explain the observed behaviour, but cannot be completely excluded on these grounds. According to our analysis, at the end of p40t115 some 70% of the total strain ($\sim$0.07) is accommodated by solution-precipitation creep. Despite considerable uncertainties associated with calculating this number, the flow law used is well established and it is unlikely that the errors are greater than 50% of the value obtained. Therefore, it is unlikely that the contribution of solution-precipitation creep is below 35%. Our analysis therefore shows that the contribution of solution-precipitation must be considerable in wet rocksalt prior to the onset of dynamic recrystallization. Such a contribution of solution-precipitation creep during deformation is not reflected by the microstructure of p40t115 (Fig. 5c), in which evidence for dislocation creep (subgrains) is widespread. Our evidence for grain boundary alignment does suggest some kind of grain boundary sliding process. On the other hand, at small strains, solution-precipitation creep will give rise to few diagnostic microstructural features, so that the microstructure is expected to be dominated by features resulting from dislocation creep. In general, determining the dominant deformation mechanism from microstructural observations is not straightforward and reliable evaluation of the contribution of grain size sensitive deformation mechanisms (e.g. solution-precipitation creep or grain boundary sliding) requires a quantitative analysis such as presented here. A similar observation was recently made in relation to natural calcite mylonites deforming by a combination of grain size sensitive (grain boundary diffusion/sliding) creep and grain size insensitive (dislocation) creep (Herwegh et al., 2005).

Overall, arithmetic mean grain size increases after the first stress peak by a factor of 3.6. Hence, the contribution of grain size sensitive solution-precipitation creep may be expected to decrease after the first peak, when fluid-assisted grain boundary migration starts. An important part of the difference in strength between the dry and wet samples is caused by the removal of strain hardening substructure by grain boundary migration. As a first-order approach, the strain rate due to solution-precipitation creep in the recrystallized material can be calculated by substituting arithmetic mean recrystallized grain size (cf. Ter Heege et al., 2005) into the flow law for solution-precipitation creep, given by Eq. (2). Dividing this strain rate by the overall creep rate yields the contribution of solution-precipitation creep to the overall creep rate of the recrystallized material. The results of this calculation for fully recrystallized samples show that up to 40% of the overall strain rate can be due to solution-precipitation creep. Of course this number is also subject to considerable uncertainty (e.g. the use of mean grain sizes and the application of the solution-precipitation flow law), but it does show that solution-precipitation creep can play an important role in the deformation of wet rocksalt, even after the onset of dynamic recrystallization.

4.3. Comparison with previous studies

The flow parameters from this study and a selection of previous studies, relevant to this study, are given in Table 2. In all studies, the flow law parameters were obtained by fitting mechanical data to a power law equation of the type given in Eq. (1). The deformation conditions imposed in the present experiments fall in the range of conditions used in the selected studies, or at least show some overlap, although confining pressures vary. The conditions in the present study correspond to the high strain rate and stress regime of Carter et al. (1993). Franssen (1994) performed unconfined experiments, predominantly at higher temperatures than in the present study, and the samples in his study are therefore absolutely dry. The stress exponent (n) for our wet material is close to the values in the other studies, except for the value found in the low strain rate and stress regime of Carter et al. (1993) and the value found by Hunsche and Hampel (1999). The variation in apparent activation energy of the different studies is more pronounced. For the relevant

deformation conditions, most of the selected studies show values for the apparent activation energy in the range of 68–98 kJ/mol, lower than the activation energy for lattice diffusion of the slowest diffusing chloride anion measured independently (205–221 kJ/mol) (see review in Franssen, 1994), or estimates of the activation energy for short-circuit diffusion through dislocation cores (pipe diffusion, 103–155 kJ/mol) (Wawersik and Zeuch, 1986; Franssen, 1994). Deviating values were found by Wawersik and Zeuch (1986) for some of the rocksalt types investigated, by Franssen (1994) for absolutely dry rocksalt and by Hunsche and Hampel (1999).

The interpretation of the mechanical behaviour in terms of deformation mechanisms using the power law creep parameters is not straightforward. In the selected studies, it is claimed that dislocation creep is controlled by climb of dislocations (Heard, 1972; Heard and Ryerson, 1986; Carter et al., 1993; Franssen, 1994) or by cross slip of dislocations (Wawersik and Zeuch, 1986; Carter et al., 1993). These claims are mainly based on comparison of the data with microphysical models for climb or cross slip-controlled creep, on comparison of apparent activation energies, and on microstructural evidence for climb and cross slip. Carter et al. (1993) found a change in rheological behaviour going from a high stress and strain rate regime to a low strain rate and stress regime, and ascribed this change to a transition from cross slip-controlled to climb controlled creep. Evidently, no consensus exists regarding the rate controlling deformation mechanism in rocksalt at conditions relevant to nature, and no satisfactory explanation has been given for the low activation energy seen in previous experiments at $T<200$ °C. None of the selected studies included solution-precipitation creep as an active deformation mechanism, although some studies argued that it may become important at lower stresses, strain rates and grain sizes (Carter et al., 1993). The low apparent activation energy obtained in the present study, and the occurrence of linear wavy substructure interpreted to be slip lines, point to cross slip-controlled dislocation creep in wet rocksalt (Wawersik and Zeuch, 1986; Carter et al., 1993), but the evidence is not conclusive. Alternatively, a low apparent activation energy could be the result of the contribution of solution-precipitation creep (activation energy 24.5 kJ/mol) to the overall creep rate of wet rocksalt. However, in materials deforming by combined grain size-sensitive and grain size-insensitive mechanisms, flow law parameters, such as apparent activation energy, depend on the characteristics of the grain size distribution of the material (Freeman and Ferguson, 1986; Wang, 1994; Ter Heege et al., 2004). Therefore, the value for the apparent activation energy does not necessarily reflect a contribution of solution-precipitation creep, and may even still be indicative of the mechanism controlling dislocation motion. Further (independent direct diffusion) studies are required to make definite conclusions regarding the microphysical processes that lead to this activation energy.

In Fig. 7, strain rates of the different studies, calculated using Eq. (1) with the flow law parameters of Table 2, are compared for 125 and 150 °C. At all relevant stresses, the flow rates of the wet samples in the present study are higher than the flow rates in virtually all other studies, i.e. the wet material is weaker than all other types of rocksalt tested except for the weakest types investigated by Wawersik and Zeuch (1986), i.e. bedded salt from the Solado formation in New Mexico. At 125 °C, the difference in strain rate between the present study and most of the other studies on 'wet' rocksalt is around a factor of 10 or, alternatively, the difference in strength is around a factor of 1.5 for the relevant range in flow stresses and strain rates. The discrepancy between the strength of rocksalt observed in the selected studies and the present study can be explained by (1) the effect of water (loss), (2) the effect of dilatancy, (3) the effect of impurities and (4) the effect of strain. A key observation related to these points is that in all the other studies, except for the study by Peach et al. (2001), grain boundary migration appears not to have occurred.

Comparison between wet and dry samples in this study shows that dry samples with a water content of ≤ 5 ppm are much stronger than wet samples (9–46 ppm water after the experiments) and that grain boundary migration does not occur in the dry samples. Evidently, water has an important effect on the strength and microstructural evolution of rocksalt. At least part of the variation in strength of the different rocksalt types investigated by Wawersik and Zeuch (1986) may be expected to be due to differences in water content. Heard (1972) reported $\sim$50% water loss during the experiments. In some cases, the water content might then fall below the critical amount making grain boundaries no longer mobile and resulting in a stronger material.

Peach and Spiers (1996) and Peach et al. (2001) found that rocksalt samples, containing $\sim$500 ppm water, can exhibit significant grain boundary dilatancy if the flow stress is more than twice the confining pressure, i.e. dilatancy occurred below a confining pressure of $\sim$18 MPa for samples deformed at 20 °C and $\sim 4\times10^{-5}$ s^{-1} and below $\sim$6.5 MPa for samples deformed at 150 °C and $\sim 4\times10^{-7}$ s^{-1}. Except for the experiments of Heard (1972), all experiments in the selected studies were performed at confining pressures of 3–21 MPa (Table 2), and several experiments were performed in the dilatant field. Therefore, dilatancy resulting in grain boundary disruption, loss of water and inhibition of grain boundary migration probably did occur. These dilatancy-related effects increase the strength of rocksalt (Peach et al., 2001) and can explain some of the differences in strength of rocksalt between the selected studies (Table 2) and the present study.

The experiment by Peach et al. (2001), indicated in Fig. 7, was performed on natural rocksalt (Asse Speisesalz) with a water content of 500 ppm at conditions where dilatancy did not occur (30 MPa confining pressure). The sample is stronger than the samples deformed in the present study, although fluid-assisted grain boundary migration was

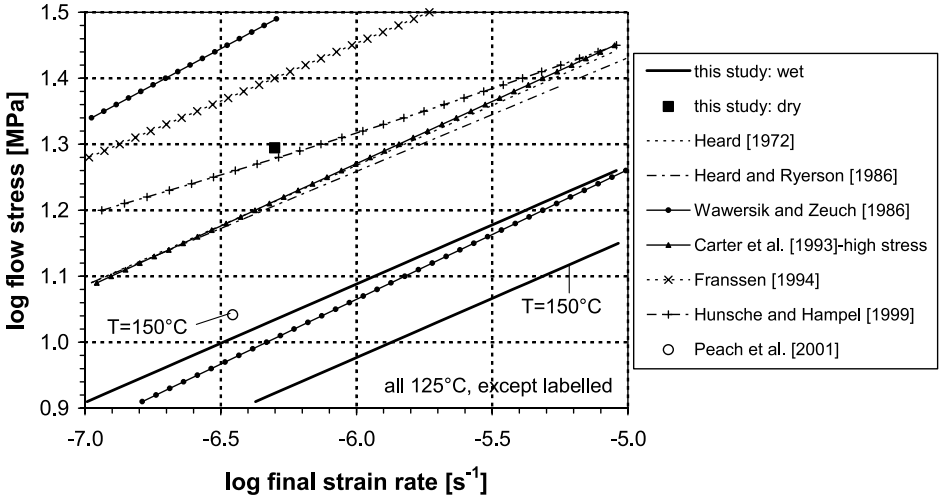

Fig. 7. Comparison of strain rates at $T = 125$ and 150 °C for dry and wet rocksalt, given by the flow laws of this study and several previous studies using the flow law parameters in Table 2. The two lines of Wawersik and Zeuch (1986) indicate the weakest and strongest type of rocksalt they investigated; all other types fall between these two bounds.

extensive. In this case, the difference in strength is most likely due to the presence of impurities in the natural rocksalt. Peach et al. (2001) reported up to 2% impurities, mainly consisting of the mineral polyhalite. Impurities can increase the strength of wet rocksalt by two mechanisms: (1) intracrystalline cation impurities decrease dislocation mobility (solid solution hardening; Heard and Ryerson, 1986) and (2) second phases on grain boundaries reduce grain boundary mobility by pinning and hence reduce recovery. Grain boundary migration is not prevented by the impurities as evidenced by the widespread evidence for migrated boundaries in the natural rocksalt samples. The higher strength of impure natural rocksalt compared to our 100% pure synthetic rocksalt shows that our flow law gives an upper limit for deformation rates of rocksalt in nature (or, alternatively, a lower limit to the strength of natural rocksalt). At least part of the variation in strength of the different rocksalt types investigated by Wawersik and Zeuch (1986) may be expected to be due to differences in composition.

Most of the selected studies in Table 2 have investigated the mechanical behaviour on the basis of uniaxial stepping experiments with limited strain in each step (typically few percent shortening) or constant stress or strain rate experiments to natural strains typically not exceeding ~0.1 (Heard, 1972; Carter et al., 1993; Hunsche and Hampel, 1999). It is obvious from Fig. 1 that mechanical steady state cannot be expected to have been reached at these low strains. This observation indicates that flow laws from the selected studies might describe transient deformation. An additional complication is that for most deformation conditions, a strain of ~0.1 is insufficient to get past the fast stress peak and to initiate significant grain boundary migration in wet rocksalt (c.f. Fig. 2). The lack of microstructural evidence for dynamic recrystallization in the selected experiments and some of the differences in strength between the selected studies and the present study can be explained by the limited strains reached in most of the selected studies.

At 125 °C, the strength of the dry samples in this study is lower than predicted by the flow law for dry rocksalt from Franssen (1994) and by the flow laws for the stronger types of natural rocksalt from Wawersik and Zeuch (1986), i.e. domal salts from the Bayou Choctaw formation in Louisiana and the Bryan Mound formation in Texas. The datapoint is very close to creep rates predicted by Hunsche and Hampel (1999) for natural rocksalt with unreported water content, deformed unconfined or at a small confining pressure of 15–20 MPa. They reported dilatation in some of the experiments (Hampel et al., 1998), which probably resulted in grain boundary disruption and water loss bringing their predictions close to ours for dry rocksalt. The experiments of Franssen (1994) were performed unconfined at high temperature and therefore the samples were absolutely dry and must have undergone some dilatancy, increasing the strength of their samples.

4.4. Flow of rocksalt in nature

Natural rocksalt generally contains inter- and intracrystalline fluid inclusions filled with brine (Roedder, 1984) and exhibits similar microstructures as observed in wet rocksalt samples investigated in this study, indicating that fluid-assisted grain boundary migration is important in nature (Urai et al., 1986, 1987; Talbot and Jackson, 1987; Spiers and Carter, 1998; Miralles et al., 2000). Considering these observations and the arguments mentioned in Section 4.3, our flow law for wet rocksalt is best suitable for describing flow of rocksalt in nature. It is unclear to what extent it is justified to apply previous flow laws for dislocation creep to nature, since these flow laws do not include the effect of dynamic recrystallization.

Application of a single power law creep equation describing multiple deformation mechanisms to natural situations is not straightforward, because the different deformation mechanisms may interact differently upon extrapolation. Therefore, extrapolation is only justified if recrystallized grain size adjusts itself so that the relative contribution of the deformation mechanisms is constant during steady state, independent of stress and temperature (cf. De Bresser et al., 2001; Ter Heege, 2002) or $C = \dot{\varepsilon}_{sp}/\dot{\varepsilon}_{dis+gbm}$ is constant, with $\dot{\varepsilon}_{dis+gbm}$ the dislocation creep rate including the effect of enhanced recovery by grain boundary migration (cf. Sections 4.1 and 4.2). If this holds, the steady-state creep rate of the dynamically recrystallizing material $\dot{\varepsilon}_{rx}$ can be written as (using Eq. (2))

$$\dot{\varepsilon}_{rx} = \dot{\varepsilon}_{sp} + \dot{\varepsilon}_{dis+gbm} = \frac{C+1}{C}\dot{\varepsilon}_{sp}$$

$$= (4.7 \pm 2.3)10^5 \frac{C+1}{C} \frac{\sigma}{TD^3} \exp\left(\frac{-24.5 \pm 1.0}{RT}\right) \quad (5)$$

where D is the mean recrystallized grain size. We have written Eq. (5) so that it only includes terms that are known from previous studies (e.g. $\dot{\varepsilon}_{sp}$—see Eq. (2)), or can be obtained from the experiments in this study (e.g. $\dot{\varepsilon}_{rx}$ and D). Note that our flow law includes a contribution of solution-precipitation creep (cf. Section 4.2) and therefore represents $\dot{\varepsilon}_{rx}$ and not $\dot{\varepsilon}_{dis+gbm}$. In a previous study, we calibrated the following mean recrystallized grain size piezometer for wet rocksalt undergoing fluid-assisted grain boundary migration (Ter Heege et al., 2005)

$$\left(\frac{D}{b}\right) = 10^{-1.55\pm0.24}\left(\frac{\sigma}{\mu}\right)^{-1.85\pm0.23} \exp\left(\frac{14.2 \pm 2.8}{RT}\right) \quad (6)$$

with D denoting mean recrystallized grain size, Burgers vector $b = 3.99 \times 10^{-4}$ μm and shear modulus $\mu = 1.5 \times 10^4$ MPa. If grain size is free to adjust itself via dynamic recrystallization, constant C can be found by substitution of this relation and the power law creep equation given in Eq. (1) with our values for the flow law parameters from Table 1 in Eq. (5)

$$C = \left[10^{-11.9\pm1.3}\mu^{5.6\pm0.7}b^3 T\sigma^{-1.0\pm1.2}\exp\left(\frac{-13 \pm 15}{RT}\right) - 1\right]^{-1} \quad (7)$$

The constant C given by Eq. (7) is subject to considerable errors, mainly as a result of propagating errors (upon substitution) associated with calibration of the piezometer and the flow law for $\dot{\varepsilon}_{rx}$. Due to the large uncertainties in Eq. (7), well-constrained values for C cannot be calculated. However, Eq. (7) does show that, within errors, there is no significant dependence of C on stress and temperature within the relevant range of deformation conditions, suggesting that the relative contributions of solution-precipitation and dislocation creep with grain boundary migration are independent of stress and temperature. These findings support the notion that rheology of wet rocksalt is confined to the boundary between the solution-precipitation and dislocation creep (with the effect of grain boundary migration) fields as hypothesized by the field boundary model of De Bresser et al. (1998, 2001). In accordance with this model, the steady-state flow of dynamically recrystallizing rocksalt can be described by a single grain size-independent power law creep equation of the type given by Eq. (1), i.e. $\dot{\varepsilon}_{rx}$ can be written in terms of the grain size-independent flow law for $\dot{\varepsilon}_{dis+gbm}$($\dot{\varepsilon}_{rx} = (C+1)\dot{\varepsilon}_{dis+gbm}$). Hence, it is justified to apply our flow law to conditions relevant for the flow of rocksalt in nature, provided it deforms at mechanical and microstructural steady state. Considering the relative low strains required to achieve (near) steady state deformation in our experiments and the high strains associated with salt tectonics (halokinesis), rocksalt in nature can generally be regarded to deform at steady state.

The analysis also shows that materials deforming by a combination of grain size sensitive (e.g. solution-precipitation) creep and grain size insensitive (e.g. dislocation) creep may show high stress exponents that do not reflect a significant contribution of the grain size sensitive deformation mechanism (with $n = 1$ or 2, cf. Eq. (2)). These findings are in agreement with previous (modelling) studies, which show that the stress exponent (and also activation energy) in materials deforming by combined grain size sensitive—grain size insensitive deformation mechanisms is dependent on the characteristics of the grain size distribution of the material (Freeman and Ferguson, 1986; Wang, 1994; Ter Heege et al., 2004).

Together with the piezometer for wet rocksalt, given by Eq. (6), our flow law can be used to fully constrain deformation of rocksalt in nature, provided the mean recrystallized grain size has been analysed and the deformation temperature is known. The piezometer gives an estimate of the flow stress associated with the deformation of the rock, which can be inserted in our flow law to give the rate of deformation (Fig. 8). For typical grain size of natural rocksalt of 5–20 mm and deformation temperatures of 50–200 °C (Urai et al., 1986; Carter et al., 1993; Spiers and Carter, 1998), the piezometer predicts flow stresses of 1.0–5.6 MPa and the flow law predicts strain rates of 7×10^{-13}–4×10^{-9} s^{-1}, depending on temperature (Fig. 8). These values agree well with estimates of flow stresses deduced from the application of relevant constitutive creep equations to natural conditions combined with structural geological studies or from the application of subgrain size piezometric relations (Jackson and Talbot, 1986; Carter et al., 1982, 1993; Spiers and Carter, 1998). Note that the reported grain sizes are mean values in these estimates. The existing piezometers for rocksalt were calibrated at high temperatures (250–790 °C) under atmospheric pressure in Argon using single crystals of halite (Guillopé and Poirier, 1979). Analogous to unconfined experiments at high temperature (e.g. Franssen, 1994), the

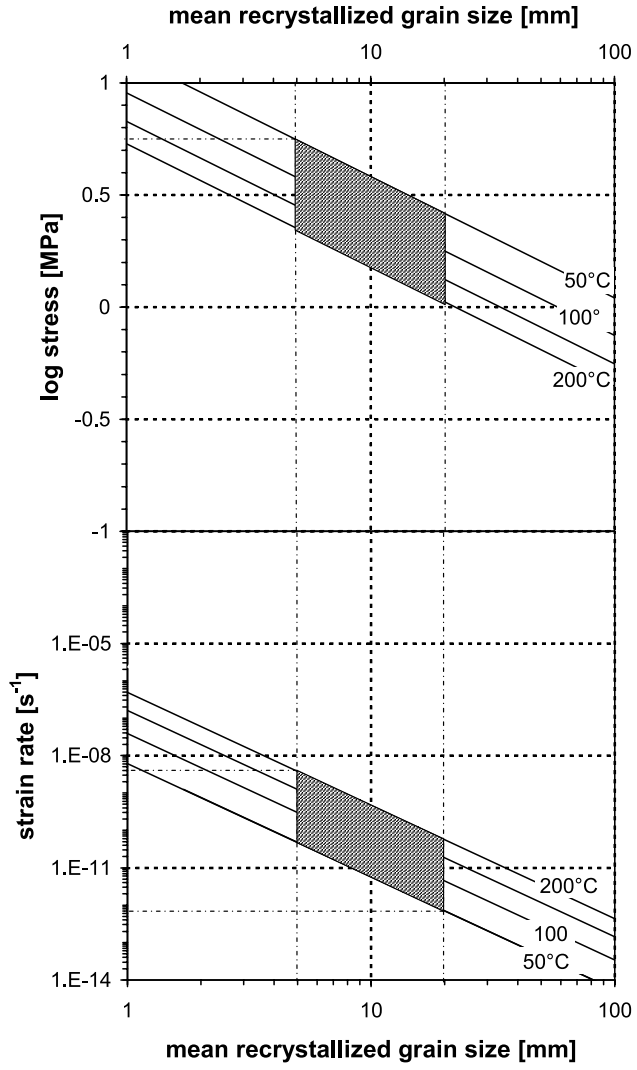

Fig. 8. Isotherms for the piezometer and estimate of flow stresses and deformation rates of natural rocksalt using the flow law calibrated in this study and the piezometer from Ter Heege et al. (2005). The ranges of flow stresses and strain rates for a realistic range in grain size and deformation temperature (shaded areas) of natural rocksalt are indicated.

grain boundaries of recrystallized grains that nucleate will therefore be absolutely dry and application of these piezometers to natural rocksalt containing fluid films at grain boundaries is probably not justified (cf. Ter Heege et al., 2005).

In Section 4.3, we showed that existing flow laws significantly underestimate the strain rate (around a factor 10 at 125 °C and relevant flow stresses in this study), mainly owing to the fact that solution-precipitation creep and fluid-assisted grain boundary migration are unaccounted for in the flow laws. Evidently, our flow law provides better constraints on flow of rocksalt in nature and will be essential for accurate modelling of salt tectonics in geo-engineering applications, such as radioactive waste disposal in salt caverns, borehole closure and closure of deep solution-mining cavities (see, e.g. Carter and Hansen, 1983; Peach, 1991; Aubertin and Hardy, 1998 and references therein).

It has often been proposed that strain localization may result from rheological weakening due to progressive removal of strain hardening substructure by grain boundary migration (e.g. Poirier, 1980; White et al., 1980; Rutter, 1998). In wet rocksalt, grain boundary migration is very rapid, allowing assessment of the effect of grain boundary migration on the flow strength. Grain boundary migration results in a change from a fully hardened microstructure to a fully recrystallized microstructure, which causes a decrease in flow stress (Fig. 1). The maximum weakening due to grain boundary migration, i.e. the difference in stress between the first stress peak and the subsequent stress minimum is limited to 15% in our experiments and decreases with decreasing strain rate and increasing temperature (Table 1, Fig. 3). We therefore conclude that rheological weakening due to progressive removal of strain hardening substructure by grain boundary migration is unlikely to produce strain localization in natural rocksalt. Considering the large difference in strength of dry and wet rocksalt (Figs. 1, 4 and 7), water weakening due to localized fluid infiltration may be a more viable candidate for initiating localized deformation. It has been shown that infiltration of meteoric water into exposed salt glaciers can greatly enhance downslope movement during rainy seasons (Talbot and Rogers, 1980). Moreover, Miralles et al. (2000) investigated rocksalt in a shear zone crosscutting neighbouring salt units with different water contents in the southern Pyrenees foreland. They found differences in deformation microstructures, related to differences in water content of the rocksalt in the units. These examples show that differences in water content, e.g. due to fluid infiltration or initially present variations, can give rise to different behaviour in natural rocksalt. Therefore, localized fluid infiltration may well cause localization of deformation in rocksalt. To investigate this further, field studies of salt tectonics should be performed, focusing on the spatial relation between water content and deformation, to test if fluids and strain remain localized during deformation.

5. Summary and conclusions

Dry ($\leq$5 ppm water) and wet (9–46 ppm water) rocksalt aggregates have been deformed to natural strains in the range of 0.1–0.7 at a strain rate of 5×10^{-7}–1×10^{-4} s^{-1}, temperature of 75–243 °C and stress of 7–22 MPa to investigate the role of water in determining the rheological behaviour and active deformation and recrystallization mechanisms:

1. At the investigated conditions, dry rocksalt shows continuous work hardening up to a strain of 0.25–0.51. Deformation occurs by dislocation creep, which is accompanied by subgrain formation. Wet rocksalt shows work hardening up to a peak stress at a strain of 0.07–0.32, followed by oscillating stress–strain

behaviour due to the occurrence of fluid-assisted grain boundary migration counteracting hardening processes. Deformation occurs by a combination of solution-precipitation and dislocation creep.

2. Dry rocksalt is stronger than the wet material at all strains investigated and deforms by a work hardening dislocation creep process. The difference in strength is up to a factor ~ 2 for temperatures of 125–175 °C, and can be explained by the absence of solution-precipitation creep and fluid-assisted grain boundary migration in dry rocksalt.
3. The (near) steady-state mechanical data obtained for wet rocksalt can be empirically described by a Dorn-type power law rate equation with $n = 5.6$ and $Q = 80$ kJ/mol. The flow law is the first to incorporate dislocation and solution-precipitation creep and the effect of fluid-assisted grain boundary migration. These deformation and recrystallization mechanisms are commonly found to be of major importance during flow of rocksalt in nature. Existing flow laws are based on experiments that do not show solution-precipitation creep or fluid-assisted grain boundary migration. In these experiments, fluid-assisted processes were most likely inhibited because of water loss or grain boundary disruption due to dilatancy, or not observed because of the low strains achieved. Therefore, strain rates predicted by these existing flow laws are much slower at similar stresses and temperatures and considerably underestimate the rate of deformation (up to a factor ~ 10 at $T = 125$ °C) or overestimate the strength (up to a factor ~ 1.5 at $T = 125$ °C) of natural rocksalt. With the flow law and piezometer for wet rocksalt, stress and strain rate associated with the deformation of natural rocksalt undergoing dynamic recrystallization can be fully constrained using an analysis of the mean grain size of the rock and an independent estimate of deformation temperature.
4. Rheological weakening due to the progressive removal of strain hardening substructure by grain boundary migration is inferred to be insufficient to produce strain localization in natural rocksalt. Instead, weakening due to localized fluid infiltration seems to be a more viable candidate for initiating localized deformation.

Acknowledgements

The authors would like to thank J.L. Liezenberg for preparing the thinsections, P. van Krieken for performing the FTIR analysis and assisting with the experiments, and G.J. Kastelein and E. de Graaff for technical assistance. C.J. Peach is gratefully acknowledged for providing additional data and samples of deformed polycrystalline halite (p40 series), stimulating discussion and technical assistance. The manuscript benefited from comments by J.L. Urai and M.R. Drury on an early version of the manuscript. We also would like to thank the referees J. Tullis and K. Kanagawa for constructive comments.

References

Aubertin, M., Hardy Jr.., H.R. (Eds.), 1998. Proceedings of the Fourth Conference on the Mechanical Behaviour of Salt Trans. Tech. Publ. Series on Rock and Soil Mechanics, 22. 658pp.

Carter, N.L., Hansen, F.D., 1983. Creep of rocksalt. Tectonophysics 92, 275–333.

Carter, N.L., Hansen, F.D., Senseny, P.E., 1982. Stress magnitudes in natural rocksalt. Journal of Geophysical Research 87, 9289–9300.

Carter, N.L., Kronenberg, A.K., Ross, J.V., Wiltschko, D.V., 1990. Control of fluids on deformation of rocks. In: Knipe, R.J., Rutter, E.H. (Eds.), Deformation Mechanisms, Rheology and Tectonics Geological Society of London Special Publication, 54, pp. 1–13.

Carter, N.L., Horseman, S.T., Russel, J.E., Handin, J., 1993. Rheology of rocksalt. Journal of Structural Geology 15, 1257–1271.

De Bresser, J.H.P., Peach, C.J., Reijs, J.P.J., Spiers, C.J., 1998. On dynamic recrystallization during solid state flow: effects of stress and temperature. Geophysical Research Letters 25, 3457–3460.

De Bresser, J.H.P., Ter Heege, J.H., Spiers, C.J., 2001. Grain size reduction by dynamic recrystallization: can it result in major rheological weakening? International Journal of Earth Sciences 90, 28–45.

Drury, M.R., Humphreys, F.J., 1988. Microstructural shear criteria associated with grain-boundary sliding during ductile deformation. Journal of Structural Geology 10, 83–89.

Franssen, R.C.M.W., 1994. The rheology of synthetic rocksalt in uniaxial compression. Tectonophysics 233, 1–40.

Freeman, B., Ferguson, C.C., 1986. Deformation mechanism maps and micromechanics of rocks with distributed grain sizes. Journal of Geophysical Research 91, 3849–3860.

Guillopé, M., Poirier, J.P., 1979. Dynamic recrystallization during creep of single-crystalline halite: an experimental study. Journal of Geophysical Research 84, 5557–5567.

Hampel, A., Hunsche, U., Weidinger, P., Blum, W., 1998. Description of the creep of rock salt with the composite model—II. Steady state creep. In: Aubertin, M., Hardy Jr.., H.R. (Eds.), Proceedings of the Fourth Conference on the Mechanical Behaviour of Salt Trans. Tech. Publ. Series on Rock and Soil Mechanics, 22, pp. 287–299.

Heard, H.C., 1972. Steady-state flow in polycrystalline halite at pressure of 2 kilobars. In: Heard, H.C., Borg, I.Y., Carter, N.L., Raleigh, C.B. (Eds.), Flow and Fracture of Rocks AGU Geophysical Monograph Series, 16, pp. 191–210.

Heard, H.C., Ryerson, F.J., 1986. Effect of cation impurities on steady-state flow of salt. In: Hobbs, B.E., Heard, H.C. (Eds.), Mineral and Rock Deformation: Laboratory Studies AGU Geophysical Monograph Series, 36, pp. 99–115.

Heilbronner, R., Bruhn, D., 1998. The influence of three-dimensional grain size on the rheology of polyphase rocks. Journal of Structural Geology 20, 695–705.

Herwegh, M., Ter Heege, J.H., De Bresser, J.H.P., 2005. Combining natural microstructures with composite flow laws: an improved approach for the extrapolation of lab data to nature. Journal of Structural Geology 27, 503–521.

Hunsche, U., Hampel, A., 1999. Rock salt—the mechanical properties of the host rock material for a radioactive waste repository. Engineering Geology 52, 271–291.

Jackson, M.P.A., Talbot, C.J., 1986. External shapes, strain rates and dynamics of salt structures. Geological Society of America Bulletin 97, 305–323.

Miralles, L., Sans, M., Pueyo, J.J., Santanach, P., 2000. Recrystallization salt fabric in a shear zone (Cardona diapir, southern Pyrenees, Spain). In: Vendeville, B., Mart, Y., Vigneresse, J.-L. (Eds.), Salt, Shale and Igneous Diapirs in and around Europe Geological Society of London Special Publication, 174, pp. 149–167.

Peach, C.J., 1991. Influence of deformation on the fluid transport properties of salt rocks. PhD Thesis. Utrecht University, Geologica Ultraiectina 77, 238pp.

Peach, C.J., Spiers, C.J., 1996. Influence of crystal plastic deformation on dilatancy and permeability development in synthetic salt rock. Tectonophysics 256, 101–128.

Peach, C.J., Spiers, C.J., Trimby, P.W., 2001. Effect of confining pressure on dilatation, recrystallization, and flow of rock salt at 150 °C. Journal of Geophysical Research 106, 13315–13328.

Poirier, J.P., 1980. Shear localization and shear instability in materials in the ductile field. Journal of Structural Geology 2, 135–142.

Raj, R., Ghosh, A.K., 1981. Micromechanical modelling of creep using distributed parameters. Acta Metallurgica 29, 283–292.

Roedder, E., 1984. The fluids in salt. American Mineralogist 69, 413–439.

Rutter, E.H., 1998. Use of extension testing to investigate the influence of finite strain on the rheological behaviour of marble. Journal of Structural Geology 20, 243–254.

Schenk, O., Urai, J.L., 2004. Microstructural evolution and grain boundary structure during static recrystallization in synthetic polycrystals of Sodium Chloride containing saturated brine. Contributions to Mineralogy and Petrology 146, 671–682.

Sellars, C.M., 1978. Recrystallization of metals during hot deformation. Philosophical Transactions of the Royal Society of London A 288, 147–158.

Senseny, P.E., Hansen, F.D., Russel, J.E., Carter, N.L., Handin, J., 1992. Mechanical behaviour of rocksalt: phenomenology and micromechanism. International Journal of Rock Mechanics 29, 363–378.

Skrotzki, W., Liu, Z.G., 1982. Analysis of the cross slip process in alkali halides. Physica Status Solidi A 73, 225–229.

Spiers, C.J., Carter, N.L., 1998. Microphysics of rocksalt flow in nature. In: Aubertin, M., Hardy Jr., H.R. (Eds.), Proceedings of the Fourth Conference on the Mechanical Behaviour of Salt Trans. Tech. Publ. Series on Rock and Soil Mechanics, 22, pp. 115–128.

Spiers, C.J., Schutjens, P.M.T.M., Brzesowsky, R.H., Peach, C.J., Liezenberg, J.L., Zwart, H.J., 1990. Experimental determination of constitutive parameters governing creep of rocksalt by pressure solution. In: Knipe, R.J., Rutter, E.H. (Eds.), Deformation Mechanisms, Rheology and Tectonics Geological Society of London Special Publication, 54, pp. 215–227.

Talbot, C.J., Jackson, M.P.A., 1987. Internal kinematics of salt diapirs. The American Association of Petroleum Geologists Bulletin 71, 1068–1093.

Talbot, C.J., Rogers, E.A., 1980. Seasonal movements in a salt glacier in Iran. Science 208, 395–397.

Ter Heege, J.H., 2002. Relationship between dynamic recrystallization, grain size distribution and rheology. PhD Thesis. Utrecht University, Geologica Ultraiectina 218, 141pp.

Ter Heege, J.H., De Bresser, J.H.P., Spiers, C.J., 2002. The influence of dynamic recrystallization on the grain size distribution and theological behaviour of Carrara marble deformed in axial compression. In: De Meer, S., Drury, M.R., De Bresser, J.H.P., Pennock, G.M. (Eds.), Deformation Mechanisms, Rheology and Tectonics: Current Status and Future Perspectives Geological Society of London Special Publication, 200, pp. 119–130.

Ter Heege, J.H., De Bresser, J.H.P., Spiers, C.J., 2004. Composite flow laws for crystalline materials with log-normally distributed grain size: theory and application to olivine. Journal of Structural Geology 26, 1693–1705.

Ter Heege, J.H., De Bresser, J.H.P., Spiers, C.J., 2005. Dynamic recrystallization of wet synthetic polycrystalline halite: dependence of grain size distribution on flow stress, temperature and strain. Tectonophysics 396, 35–57.

Tullis, T.E., Horowitz, F.G., Tullis, J., 1991. Flow laws of polyphase aggregates from end-member flow laws. Journal of Geophysical Research 96, 8081–8096.

Urai, J.L., 1983. Water assisted dynamic recrystallization and weakening in polycrystalline bischofite. Tectonophysics 96, 125–157.

Urai, J.L., 1985. Water-enhanced dynamic recrystallization and solution transfer in experimentally deformed carnallite. Tectonophysics 120, 285–317.

Urai, J.L., Spiers, C.J., Zwart, H.J., Lister, G.S., 1986. Weakening of rock salt by water during long-term creep. Nature 324, 554–557.

Urai, J.L., Spiers, C.J., Peach, C.J., Franssen, R.C.M.W., Liezenberg, J.L., 1987. Deformation mechanisms operating in naturally deformed halite rocks as deduced from microstructural investigations. Geologie en Mijnbouw 66, 165–176.

Wang, J.N., 1994. The effect of grain size distribution on the rheological behavior of polycrystalline materials. Journal of Structural Geology 16, 961–970.

Watanabe T., Peach C. J., 2002. Electrical impedance measurement of plastically deforming halite rocks at 125°C and 50MPa. Journal of Geophysical Research 107, 2004, doi.10.1029/2001JB000204

Wawersik, W.R., Zeuch, D.H., 1986. Modelling and mechanistic interpretation of creep of rock salt below 200 °C. Tectonophysics 121, 125–152.

White, S.H., Burrows, S.E., Carreras, J., Shaw, N.D., Humphreys, F.J., 1980. On mylonites in ductile shear zones. Journal of Structural Geology 2, 175–187.